Synthesis of Ternary Nitrides from Intermetallic Precursors: Modes of Nitridation in Model Cr_3Pt Alloys To Form Cr_3PtN Antiperovskite and Application to Other Systems

Michael P. Brady,*,† Sarah K. Wrobel,‡ Tom A. Lograsso,§ E. Andrew Payzant,† David T. Hoelzer,† Joseph A. Horton,† and Larry R. Walker†

Oak Ridge National Laboratory, Oak Ridge, Tennessee 37831-6115, University of Tennessee, Knoxville, Tennessee 37996-2200, and Ames Laboratory, Iowa State University, Ames, Iowa 50011

Received October 1, 2003. Revised Manuscript Received March 3, 2004

The use of intermetallic alloy precursors is explored as a new means to synthesize complex transition and refractory metal nitrides, carbides, and related phases. The conditions under which model single-phase Cr_3Pt and two-phase Cr_3Pt-dispersed Cr alloys form Cr_3PtN antiperovskite when thermally nitrided were studied. Phenomenological experiments suggest that the key variable to achieving single-phase Cr_3PtN surface layers is the Cr_3Pt phase composition. In two-phase β-Cr−Cr_3Pt alloys, the formation of single-phase Cr_3PtN at Cr_3-Pt precipitates by in-place internal nitridation was found to be a strong function of the size of the Cr_3Pt dispersion in the microstructure. Nanoscale Cr_3Pt dispersions were readily converted to near single-phase Cr_3PtN, whereas nitridation of coarse Cr_3Pt particles resulted in a cellular or discontinuous-type reaction to form a lath mixture of Cr_3PtN and a more Cr-rich Cr_3Pt or β-Cr. The potential for using such external/internal oxidation phenomena as a synthesis approach to layered or composite surfaces of ternary ceramic phases (nitrides, carbides, borides, etc.) of technological interest such as the Ti_3AlC_2 phase, bimetallic nitride, and carbide catalysts (Co_3Mo_3N and Co_3Mo_3C and related phases), and magnetic rare earth nitrides ($Fe_{17}Sm_2N_x$ or $Fe_{17}Nd_2N_x$) is discussed.

Introduction

Ternary and higher order (complex) transition and refractory metal nitrides, carbides, and so forth exhibit unique combinations of interesting and potentially useful magnetic, electrical, catalytic, optical, chemical, and mechanical behaviors. However, they have not been as well-explored as complex oxide phase systems.[1,2] A major barrier to the study of complex nitrides, and ultimately to technological realization of their unique properties, is a lack of available synthesis techniques.[1,2] The difficulty in synthesis of complex nitride compounds can be traced to bonding aspects of nitrogen, the large energy barrier for the dissociation of atomic nitrogen to N^{3-}, and the tendency of many nitrides to decompose at high temperatures.[1−3]

Ammonolysis of complex oxide precursors[4,5] has been identified as a promising approach to complex nitride synthesis, including new complex transition metal nitride phases (e.g., Fe_3Mo_3N from ammonolysis of $FeMoO_4$[6]). The advantage of this approach is that the metals are already mixed at the atomic level in the precursor oxide structure.[6] Recently, we proposed that intermetallic compounds could also be used as precursors for the formation of complex transition metal ceramic phase surfaces (nitrides, carbides, and so forth), taking advantage of the bonding and/or structure characteristics of the intermetallic compound as a precursor to form the ternary ceramic phase.[7] A benefit of this approach is the potential to use metal stoichiometries and structures in the intermetallic precursor systems that are different than those available in oxide precursor systems, with the goal of synthesizing new ternary ceramic phases not achievable via oxide precursors. As with oxides, this approach can be used with single-phase intermetallic precursor powders as a starting point to yield single-phase surfaces. However, the potential also exists to start with powders, consolidated bulk materials, or coatings and form dispersed composite near-surface structures of ternary ceramic phases by using intermetallic precipitates formed in precursor two-phase alloy structures as a template (i.e., take advantage of

* To whom correspondence should be addressed. E-mail: bradymp@ornl.gov.
† Oak Ridge National Laboratory.
‡ University of Tennessee.
§ Iowa State University.

(1) Niewa, R.; DiSalvo, F. J. *Chem. Mater.* **1998**, *10*, 2733.
(2) Gregory, D. H. *J. Chem. Soc. Dalton Trans.* **1999**, *3*, 259.
(3) zur Loye, H. C.; Houmes, J. D.; Bem, D. S. In *The Chemistry of Transition Metal Carbides and Nitrides*; S. T. Oyama, Ed.; Chapman and Hall: London, 1996; p 154.
(4) Elder, S. H.; Doerrer, L. H.; DiSalvo, F. J.; Parise, J. B.; Guyomard, D.; Tarascon, J. M. *Chem. Mater.* **1992**, *4*, 928.
(5) Marchand, R.; Laurent, Y.; Guyader, J.; L'Haridon, P.; Verdier, J. *Eur. Ceram. Soc.* **1991**, *8*, 197.
(6) Bem, D. S.; Gibson, C. P.; zur Loye, H.-C. *Chem. Mater.* **1993**, *5* (4), 397.
(7) Brady, M. P.; Hoelzer, D. T.; Payzant, E. A.; Tortorelli, P. F.; Horton, J. A.; Anderson, I. M.; Walker, L. R.; Wrobel, S. K. *J. Mater. Res.* **2001**, *16* (10), 2784.

10.1021/cm034942p CCC: $27.50
Published on Web 04/09/2004

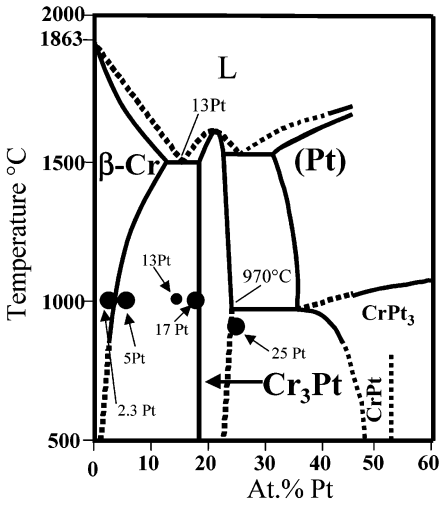

Figure 1. Schematic Cr-rich portion of the Cr−Pt phase diagram (after ref 11). The phase equilibria in the Pt-rich portions of the phase diagram are not well-defined.

metallurgical and microstructural variables that can be manipulated in the precursor alloy).

This was demonstrated for a two-phase Cr_3Pt-dispersed Cr alloy, 95Cr-5Pt atomic percent (at. %), where the Cr_3PtN antiperovskite phase[8] was formed in situ at Cr_3Pt precipitate sites in the precursor alloy by the in-place form[9,10] of internal nitridation.[7] This system was selected as a model system for study due to the high permeability of nitrogen in Cr, which favors internal modes of nitridation, the availability of a precipitation reaction to form Cr_3Pt, and the existence of the Cr_3PtN antiperovskite nitride phase. The goal of the present work was to further explore the mechanism of nitridation in the β-Cr−Cr_3Pt system and elucidate the conditions under which Cr_3PtN is formed, as a basis for guiding application of this synthesis method to other systems.

Experimental Section

Alloy Manufacture. Small 50−60-g castings of single-phase Cr_3Pt (83Cr-17Pt, 75Cr-25Pt), two-phase Cr_3Pt-dispersed Cr (95Cr-5Pt), and single-phase β-Cr (97.7Cr-2.3Pt) alloys (Figure 1) were prepared by arc melting and drop casting in a chilled copper mold. The compositions of the Cr_3Pt and β-Cr alloys were selected to extend slightly into their respective adjacent two-phase fields to allow comparison of behavior at fixed initial Cr and Pt activities and are referred to as "single phase" for convenience. The Cr_3Pt phase field ranges from Cr-rich compositions in the range of ~82Cr-18Pt in equilibrium with β-Cr to near stoichiometric Cr_3Pt of composition ~75Cr-25Pt, in equilibrium with the more Pt-rich phases (Figure 1). Therefore, two single-phase Cr_3Pt alloys were studied: 83Cr-17Pt (Cr-rich, just inside the $Cr_3Pt + \beta$-Cr two-phase field) and 75Cr-25Pt (just past the Pt-rich boundary of the Cr_3Pt phase field).

The 83Cr-17Pt, 95Cr-5Pt, and 97.7Cr-2.3Pt alloys were heat-treated in a vacuum at 1350 °C for 8 h, cooled to 1050 °C, held for 12 h, and then furnace-cooled. This treatment was selected to bring the 95Cr-5Pt alloy, in particular, into the single-phase β-Cr field and then precipitate out the Cr_3Pt phase. The 75Cr-25Pt alloy was heat-treated at 950 °C for 24 h to maximize the volume fraction of Cr_3Pt in the microstructure (see Figure 1) and then furnace-cooled.

To explore variations of the Cr_3Pt-dispersed Cr microstructure, single crystals of 95Cr-5Pt and directionally solidified (DS) 87Cr-13Pt at. % β-Cr−Cr_3Pt eutectic were also grown. The single crystals made from 95Cr-5Pt were subsequently heat-treated in the same manner as the as-cast 95Cr-5Pt. The alloys were prepared as either fingers, approximately 1 cm in diameter and 7−10 cm long, for further processing by arc-zone refining, or as chill-cast rods for directional solidification. The arc-zone refining[12] was conducted using growth rates of 6 and 12.5 mm/h at 14 V and 240 A. Directional solidification was conducted in a Bridgman crystal growth configuration using alumina crucibles. Operating temperatures were approximately 150 °C above the melting point and solidification rates of 10 mm/h were used for single-crystal growths and 100 mm/h for directional growths. Following fabrication, individual single crystals of 95Cr-5Pt alloy were oriented to the principal crystallographic axis using the back reflection Laue method and were harvested from the as-grown ingots by an electrical discharge machine (EDM) to yield (100) and (111) orientations. Compositional profiles of the single-crystal portions of the samples were measured both longitudinally along the ingot as well as radially across the diameter for each alloy. Significant chemical segregation in both directions was apparent. This was likely due to liquid convective flows driven by the large density differences between Cr and Pt. These compositional changes were taken into account when extracting crystals from the ingots to achieve nominal 95Cr-5Pt samples.

Nitridation. Disk-shaped alloy specimens of approximately 12−13-mm diameter and 1−1.5-mm thickness were polished to a 600 grit finish using SiC paper. The samples were hung in a molybdenum wire cage in a vertical alumina tube furnace at a pressure of 10^{-7}atm. High-purity nitrogen at 1 atm was back-flowed through the furnace for 2 h at room temperature. The flow was then shut off and the furnace temperature was raised to 1000 °C and held for 1−100 h, followed by furnace cooling to room temperature in the nitrogen. The furnace reached the nitriding temperature in approximately 4 h and cooled to below 500 °C in about 30 min, with an additional ~6 h to reach room temperature. (The 75Cr-25Pt alloy was nitrided at 950 °C rather than 1000 °C to maximize the volume fraction of Cr_3Pt and to keep the stoichiometry of the Cr_3Pt phase as close to 3Cr:1Pt as possible; see Figure 1.)

Characterization. Nitrided samples were characterized by scanning electron electron microscopy (SEM) and X-ray diffraction (XRD) using Cu Kα radiation. Details of the identification of Cr_3PtN are provided in ref 7. Select samples also were characterized by electron probe microanalysis (EPMA) using pure element standards for Cr and Pt, a BN standard for N, and an Al_2O_3 standard to check for O. The reported compositions typically reflect an average of 3−5 points. Unless otherwise stated, phase identification was made from a combination of the XRD and EPMA data.

Results

Cr_3Pt: 75Cr-25Pt and 83Cr-17Pt Alloys. The microstructure of the 75Cr-25Pt alloy nitrided at 950 °C for 24 h is shown in Figure 2. It consisted of a ~20-μm-thick single-phase external layer of Cr_3PtN of composition 65Cr-20Pt-15N, overlying a metallic Pt-enriched layer (white) of composition 61Cr-39Pt. The Pt-enriched phase in this alloy was likely CrPt or $CrPt_3$, based solely on composition (phase equilibria in the Pt-rich regions of the Cr−Pt system are not well defined; see Figure 1). The underlying alloy consisted of a Cr_3Pt matrix (dark) of composition 77Cr-23Pt, with second-phase regions of the Pt-enriched phase of composition 65Cr-

(8) Nardin, M.; Lorthioi, G.; Barberon, M.; Madar, R.; Fruchart, E.; Fruchart, R. *C. R. Acad. Sci. Paris* **1972**, *274*, 2168.
(9) Gesmundo, F.; Gleeson, B. *Oxid. Met.* **1995**, *44*, 211.
(10) Gesmundo, F.; Niu, Y.; Viani, F. *Oxid. Met.* **1995**, *43*, 379.
(11) Venkatraman, M.; Neumann, J. P. In *Binary Alloy Phase Diagrams*, 2nd ed.; T. B. Massalski, Ed.; ASM International: Materials Park, OH, 1990; Vol. 2.
(12) Lograsso, T. A.; Schmidt, F. A. *J. Cryst. Growth* **1991**, *110*, 363.

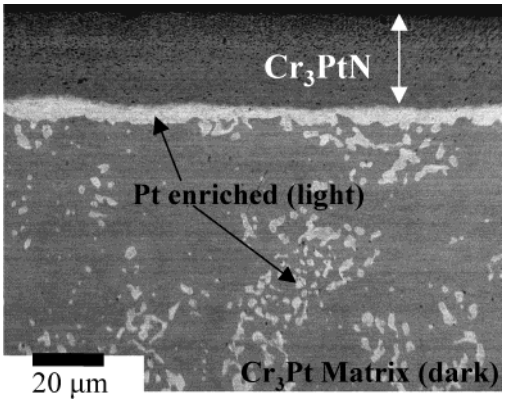

Figure 2. SEM cross section of 75Cr-25Pt after 24 h at 950 °C in N_2.

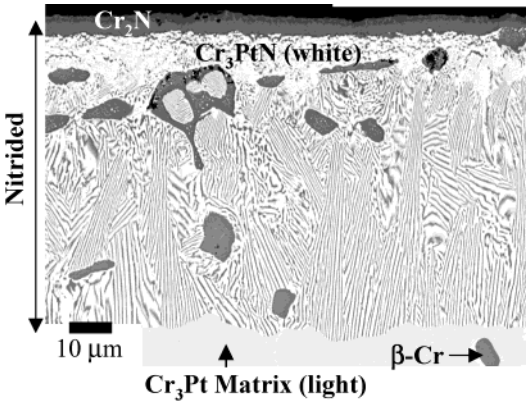

Figure 3. SEM cross section of 83Cr-17Pt after 24 h at 1000 °C in N_2.

35Pt. It should be noted that, for all alloys studied, the alloy regions underlying the nitride zones shown in the micrographs presented were representative of the initial alloy microstructures; that is, the thermal aspects of the nitridation treatment did not alter them.

The microstructure of the 83Cr-17Pt alloy nitrided at 1000 °C for 24 h (Figure 3) was markedly different than that of nitrided 75Cr-25Pt (Figure 2). It consisted of a ~ 5-μm-thick external layer of Cr_2N of composition ~70Cr-30N (trace amounts of CrN and Cr_2O_3 may also have been present at the surface), followed by a layer consisting primarily of Cr_3PtN (white), with a composition of 63Cr-19Pt-18N at. %. The region below had a complex lath structure consisting of at least two phases. Referring to Figure 3, the white lath phase had a composition of 65Cr-18Pt-17N at. %, consistent with the Cr_3PtN phase, and the dark lath phase exhibited compositions in the range (75−88)Cr-(10−17)Pt-(1−9)N. The size of the microstructure in these regions was so fine that the EPMA analysis should be considered semiquantitative due to the likelihood of beam overlap with adjacent phase(s); this is particularly the case for the dark lath phase. On the basis of the available data, the dark lath phase was Cr-rich and nitrogen-deficient relative to the Cr_3PtN and was likely β-Cr or a Cr-rich Cr_3Pt phase extension into the Cr−Pt−N system. (The presence of both β-Cr and Cr_3Pt phases in other regions of the microstructure negated a definitive identification of this Cr-rich phase by bulk XRD). The unreacted Cr_3Pt matrix just beneath this zone had a composition of 83.5Cr-16.5Pt, consistent with the nominal bulk alloy composition of 83Cr-17Pt.

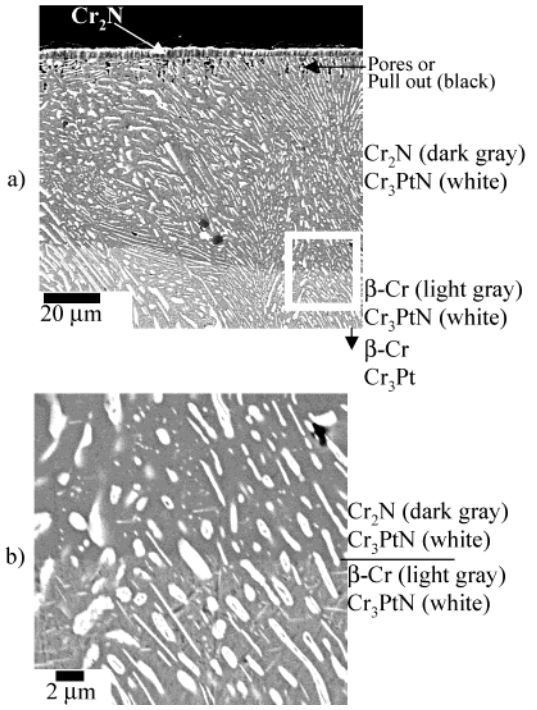

Figure 4. SEM cross sections of cast and heat-treated 95Cr-5Pt at. % after 24 h at 1000 °C in N_2 (from ref 7). (a) Low-magnification overview; (b) high-magnification view of boxed region in (a).

***β*-Cr+ Cr_3Pt: 95Cr-5Pt and 87Cr-13Pt Alloys.** Cross-section SEM micrographs for cast and heat-treated 95Cr-5Pt after 24 h of nitridation at 1000 °C are shown in Figure 4 (from ref 7). The microstructure consisted of three zones: a 3-μm Cr_2N external scale of composition 74Cr-26N, a 75-μm-thick two-phase zone of Cr_2N (dark gray matrix) of composition 69Cr-1Pt-30N and Cr_3PtN (white) of composition 65Cr-13Pt-22N, formed by in-place internal nitridation of the β-Cr and Cr_3Pt phases, respectively, and a third zone of an additional ~100-μm deep containing Cr_3PtN (white) of composition 69Cr-16Pt-15N, formed by in-place internal nitridation of Cr_3Pt, in an unreacted matrix of β-Cr of composition 99Cr-1Pt. Characteristic of in-place internal reactions, the nitrided zone followed/mirrored the underlying two-phase alloy microstructure. The composition of the Cr_3Pt phase away from the reaction zone in the bulk of the alloy was approximately ~86Cr-14Pt. (The compositions of the Cr_2N and Cr_3PtN should be considered semiquantitative due to beam overlap resulting from the fine size of the phase regions.) Most of the nitrided Cr_3Pt particles (white) appeared to be single-phase Cr_3PtN (Figure 4b). However, some of the nitrided Cr_3Pt particles also contained a small "sliver" of a dark, Cr-rich second phase. These "slivers" were likely β-Cr based or a Cr-rich $Cr_3Pt(N)$ phase extension into the Cr−Pt−N system, similar to that observed in the nitrided 83Cr-17Pt alloy (Figure 3). Attempts to *definitively* capture and identify these features in a TEM section were not successful due to their low volume fraction and the inability to rule out that the specific feature under analysis was not an extension from an adjacent region of the microstructure, as the β-Cr and Cr_3PtN phases were already present throughout the area of interest.

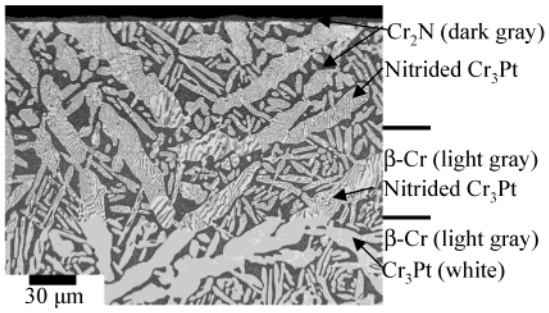

Figure 5. SEM cross section of DS 87Cr-13Pt at. % after 24 h at 1000 °C in N_2.

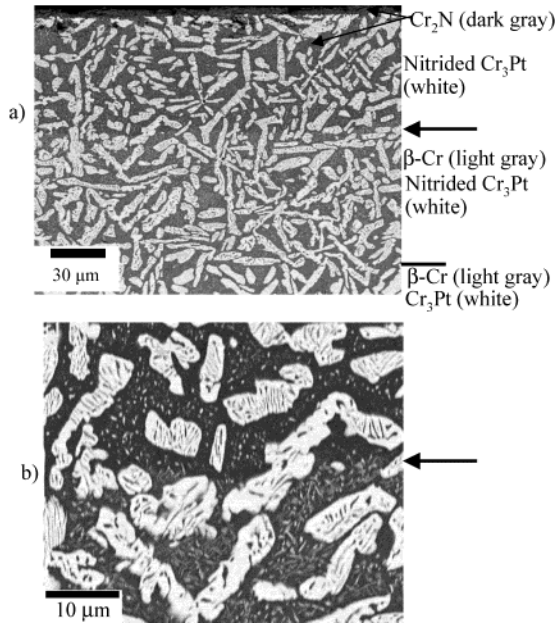

Figure 6. SEM cross sections of (100) 95Cr-5Pt after 24 h at 1000 °C in N_2. (a) Low-magnification overview; (b) higher magnification view of the Cr_2N/β-Cr interface (marked by arrow).

Nitridation of the DS 87Cr-13Pt eutectic alloy (Figure 5) yielded qualitatively comparable microstructural features to that observed in nitrided cast 95Cr-5Pt. The microstructure consisted of an external Cr_2N scale overlying an in-place internally nitrided subscale. The Cr_3Pt phase regions were nitrided to a greater depth than the β-Cr phase (as was observed in 95Cr-5Pt). However, unlike the cast 95Cr-5Pt alloy, the Cr_3Pt phase regions did not nitride to form nearly single-phase Cr_3PtN. Rather, the Cr_3Pt regions, which were much coarser than in the cast 95Cr-5Pt, reacted to form a complex lath structure of Cr_3PtN and a more Cr-rich phase, similar to that exhibited by the single-phase Cr-rich Cr_3Pt alloy 83Cr-17Pt (Figure 3).

A comparable nitrided microstructure was also observed for the (100) orientated single-crystal precursor 95Cr-5Pt (Figure 6), with the Cr_3Pt phase regions (which were again coarser than those in cast 95Cr-5Pt) nitrided to form a complex lamellar structure of Cr_3PtN and a more Cr-rich phase. In contrast, the (111)-oriented single-crystal precursor 95Cr-5Pt (Figure 7) yielded a very fine, sub-micrometer/nanoscale dispersion of Cr_3Pt in β-Cr; with single-phase Cr_3PtN observed at Cr_3Pt sites on nitridation (Figure 7) rather than the complex lath structure observed for the nitrided DS 87Cr-13Pt and the (100) 95Cr-5Pt.

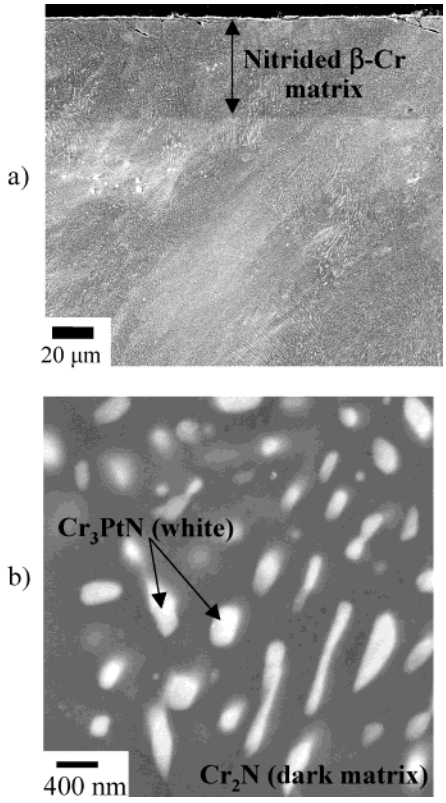

Figure 7. SEM cross section of (111) 95Cr-5Pt after 24 h at 1000 °C in N_2. (a) Overview of nitrided zone; (b) high-magnification view of the nitrided zone.

***β*-Cr: 97.7Cr-2.3Pt Alloy.** Cross-section SEM micrographs of the single-phase β-Cr alloy Cr-2.3Pt nitrided for 24 h at 1000 °C are shown in Figure 8. The microstructure consisted of an external layer of Cr_2N overlying a nitride subscale consisting of a Cr_2N matrix and a fine dispersion of Cr_3PtN. At the Cr_2N/β-Cr matrix interface, the morphology of the second phase changed from spherical Cr_3PtN to a fine, acicular morphology, with a light contrast in the SEM image consistent with Cr_3Pt. This change in second phase dispersion morphology strongly suggests that in-place internal nitridation did not occur, and it is considered likely that the acicular Cr_3Pt was not present in the microstructure of the alloy at the nitridation temperature of 1000 °C, but rather formed during cooling (solubility of Pt in the β-Cr phase decreases with decreasing temperature; see Figure 1). Both of these features (spherical Cr_3PtN and acicular Cr_3Pt) were evident in the Cr_2N/β-Cr phase regions in the two-phase β-Cr + Cr_3Pt alloys—best seen, for example, in the nitrided microstructure of the (100) Cr-5Pt (Figure 6b).

Nitridation Kinetics. Nitridation weight changes after 1, 24, and 100 h of nitridation at 1000 °C are summarized in Figure 9a for cast 83Cr-17Pt, 95Cr-5Pt, and 97.7Cr-2.3Pt. These measurements were taken from individual samples and not in situ thermogravimetry. Average depth of nitridation of the Cr_3Pt matrix for 83Cr-17Pt and the β-Cr matrix for 97.7Cr-2.3 and 95Cr-5Pt are summarized in Figure 9b. (Note that, in 95Cr-5Pt, the Cr_3Pt second phase was nitrided to a greater depth than the β-Cr matrix phase). No significant trends are obvious; this is not surprising given the complexity of the nitrided microstructures.

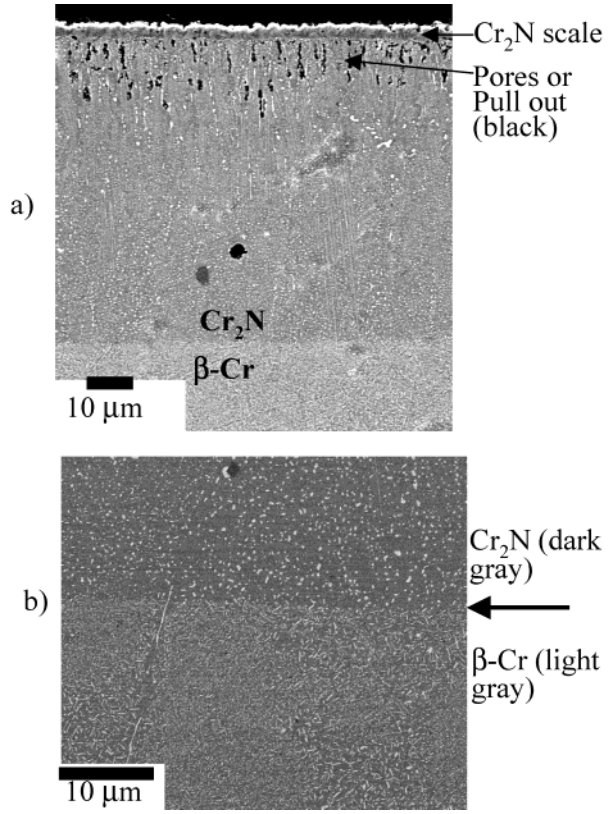

Figure 8. SEM cross sections of 97.7Cr-2.3Pt after 24 h at 1000 °C in N_2. (a) Overview of nitrided zone; (b) higher magnification view of Cr_2N/β-Cr interface. Note the change in morphology of the fine white dispersions from spherical (Cr_3PtN) in the Cr_2N region to acicular (Cr_3Pt) in the β-Cr region.

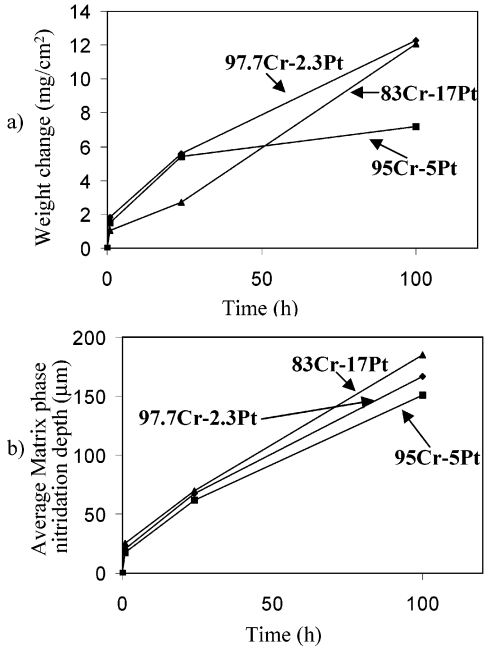

Figure 9. Nitridation data for cast and heat-treated 97.7Cr-2.3Pt, 95Cr-5Pt, and 83Cr-17Pt nitrided for 1, 24, and 100 h at 1000 °C in N_2. (a) Specific weight change; (b) depth of nitridation of the alloy matrix phase: β-Cr for 97.7Cr-2.3Pt and 95Cr-5Pt and Cr_3Pt for 83Cr-17Pt. (Note that the relatively low weight gain for the 100-h exposed 95Cr-5Pt sample was likely the result of run to run scatter; a similar series of samples exposed at 800 °C did not show this effect).

Discussion

Phase composition in single-phase Cr_3Pt alloys and dispersion size in Cr_3Pt-dispersed Cr alloys played a major role in determining whether single-phase (or near single phase) Cr_3PtN was formed. It is hypothesized that both of these phenomenon are linked to the requirements of the Cr_3PtN antiperovskite stoichiometry. The Cr_3PtN structure requires a ~3Cr:1Pt ratio. However, the intermetallic Cr_3Pt phase has a rather wide solubility range (Figure 1), and the composition in equilibrium with the β-Cr phase, ~82Cr-18Pt, is highly Cr-rich, with a Cr:Pt ratio of almost 5:1. To form Cr_3PtN, the 83Cr-17Pt alloy must give up the excess Cr. This happened during the initial stages of nitridation via the formation of an external Cr_2N scale, which allowed the formation of an underlying layer of nearly single-phase Cr_3PtN (Figure 3). At the nitride subscale reaction front, the reaction then proceeded by a discontinuous or cellular type transformation, driven by the rejection of excess Cr to form Cr_3PtN, whereby a lath structure of Cr_3PtN and a more Cr-rich phase was formed. In contrast, the Cr_3Pt phase in 75Cr-25Pt possessed nearly the same Cr:Pt stoichiometry as the Cr_3PtN phase, and an essentially single-phase layer of Cr_3PtN was formed (Figure 2).

In two-phase Cr_3Pt-dispersed β-Cr alloys, the Cr_3Pt phase is very Cr-rich and would be expected to behave locally as did the single-phase Cr_3Pt alloy 83Cr-17Pt, and exhibit a discontinuous type reaction yielding a local lath structure of Cr_3PtN and a Cr-rich phase. This was in fact observed for the DS 87Cr-13Pt eutectic alloy (Figure 5) and the (100) Cr-5Pt (Figure 6). However, such a microstructure was generally not observed for most of the fine dispersions present in cast 95Cr-5Pt from our original study (Figure 4) or in the (111) 95Cr-5Pt in the present work, which contained nanoscale dispersions of Cr_3Pt (Figure 7). It is hypothesized that the rejected Cr from these fine Cr_3Pt dispersions was accommodated by the surrounding β-Cr matrix. This interpretation suggests a critical diffusion distance relative to the Cr_3Pt dispersion size. Larger Cr_3Pt phase regions require a greater distance over which the excess Cr must diffuse out of the Cr_3Pt particle and into the β-Cr matrix during nitridation to form Cr_3PtN. As a result, if the Cr_3Pt region is too coarse, some of the excess Cr is unable to diffuse out to the β-Cr matrix and remains in the particle core forming the Cr-rich second-phase regions (Figure 10).

The Cr_3PtN phase also formed during nitridation of the single-phase β-Cr alloy 97.7Cr-2.3Pt, seemingly without the presence of Cr_3Pt precursor precipitates (i.e., not by an in-place internal reaction process). Rather, the Cr_3PtN appeared to form at the temperature by classical internal nitridation, although it is also possible that it precipitated out from a Cr−Pt−N solid solution on cooling. By either route, this result strongly suggests that Cr_3PtN is more thermodynamically stable than Cr_2N. Kosec et al.[13] reported a similar pattern of behavior for the formation of Ag_2TeO_3 by in-place internal oxidation of Ag_2Te particles in a two-phase Ag(Te) + Ag_2Te alloy and by classical internal oxidation of the Ag(Te) solid solution matrix to form Ag_2TeO_3.

(13) Kosec, L.; Roth, J.; Bizjak, M.; Anžel, I. *Oxid. Met.* **2001**, *56* (5/6), 395.

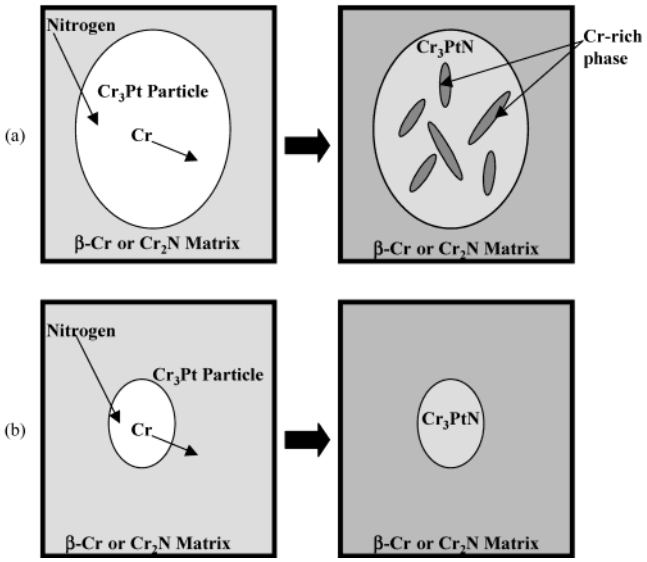

Figure 10. Schematics showing the proposed role of Cr_3Pt dispersion size on nitridation in Cr_3Pt-dispersed Cr alloys, in which the formation of single-phase Cr_3PtN required rejection of excess Cr to the matrix phase. (a) Coarse Cr_3Pt and (b) fine Cr_3Pt.

As a synthesis approach, oxidation (nitridation, carburization, etc.) reactions are a rapid and inexpensive route to forming near-surface ceramic phase structures on or in metallic substrates. Thermal oxidation of metallic-bearing precursors has been successfully exploited for the synthesis of thick film (oxide superconductors) and bulk complex ceramics (e.g., refs 14 and 15). However, in general, it has proven difficult to directly and controllably form complex ceramic phases via gas reactions because of the differences in the availability and thermodynamic stability of the metal components in the metallic precursor alloy. This is especially true for internal reactions, for which the formation of simple (binary) ceramic dispersions at size ranges from nanoscale to micrometer scale is well-established. Complex ceramic phase formation by internal reactions also has been observed, although usually as a result of subsequent solid-state reactions of an initially formed simple ceramic phase with the matrix alloy [e.g., ref 16].

The use of intermetallic precursors appears to hold promise as a method to synthesize complex ceramic phase near-surface structures by oxidation reactions, especially when needed in dispersed composite arrangements by use of in-place internal oxidation phenomena in two-phase alloys. The Cr_3PtN phase was formed from nitridation of Cr_3Pt. However, Cr_3PtN was also formed by nitridation of β-Cr solid solution, ostensibly due to the presumed greater thermodynamic stability of Cr_3PtN compared to Cr_2N. This behavior may reflect the energetic tendency of Cr and Pt to want to combine as an intermetallic phase, even when sufficient Pt to precipitate out Cr_3Pt is not present. This speculation suggests exploration of systems with dilute solid solutions in equilibrium with intermetallic phases as a basis

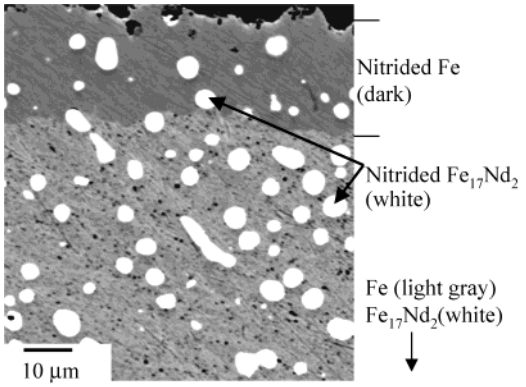

Figure 11. SEM cross section of 99Fe-1Nd after 8 h at 575 °C in NH_3.

to form complex ceramic phases. Structural relationships between parent phase and desired complex ceramic phase may also play a major role, and it is likely that complex interstitial nitride and carbide and related phases will be particularly amenable to this approach.

Extension to other systems may be possible with further understanding. For example, $R_2Fe_{17}N_x$ (R = Sm, Nd, etc) interstitial phases have been of great recent interest for magnetic applications.[17−19] These phases have typically been formed by nitridation of intermetallic powders of R_2Fe_{17} phases, but have proven difficult to synthesize and consolidate, especially into dispersed composite arrangements for technological application, and in the nanoscale-size regime needed to optimize magnetic behavior.[17−19] Figure 11 shows preliminary results for the nitridation of cast and heat-treated 99Fe-1Nd at. %. This alloy was heat-treated at 1100 °C for 12 h followed by 800 °C for 24 h to produce a microstructure of $Fe_{17}Nd_2$ dispersed in Fe and then nitrided at 575 °C for 8 h in NH_3. The nitrided microstructure consisted of two zones, an outer layer of 82Fe-18N at. %, consistent with Fe_4N, containing single-phase dispersions of composition (65−70)Fe-7Nd-(20−28)N at. %, consistent with $Fe_{17}Nd_2N_x$ interstitial phase (phase identification surmised solely from SEM and EPMA analysis). Underlying this layer was a zone of Fe metal containing the $Fe_{17}Nd_2N_x$. This microstructure is consistent with in-place internal nitridation of the Fe matrix and $Fe_{17}Nd_2$ precipitates, in a manner analogous to that for the Cr_3Pt dispersed Cr alloys. For technological use, it will be necessary to form the initial $Fe_{17}Nd_2$ precipitates at a much finer scale, which may be achievable by rapid solidification or the use of metastable Fe(Nd) thin film precursors. These initial results for Fe−Nd point to the potential of this method to synthesize structures and compounds of technological interest, beyond the model Cr_3Pt/Cr_3PtN system.

One could also envision synthesis of near-surface layers or dispersions of ternary nitride or carbide phases with interesting and unique mechanical and physiochemical properties such as Ti_3AlC_2[20] by carburization

(14) Yurek, G. J.; VanderSande, J. B.; Wang, W.-X.; Rudman, D. A. *J. Electrochem. Soc.* **1987**, *10*, 2635.
(15) Sandhage, K. H.; Allameh, S. M.; Kumar, B.; Schmutzler, H. J.; Viers, D.; Zhang, X. D. *Mater. Manuf. Processes* **2000**, *15* (1), 1.
(16) Megusar, J.; Meier, G. H. *Metall. Trans. A* **1976**, *7*, 1133.
(17) Coey, J. M. D.; Lawler, J. F.; Sun, H.; Allan, J. E. M. *J. Appl. Phys.* **1991**, *69* (5), 3007.
(18) McHenry, M. E.; Laughlin, D. E. *Acta Mater.* **2000**, *48*, 223.
(19) Machida, K; Adachi, G. In *The Chemistry of Transition Metal Carbides and Nitrides*; S. T. Oyama, Ed.; Chapman and Hall: London, 1996; p 191.
(20) Tzenov, N. V.; Barsoum, M. W. *J. Am. Ceram. Soc.* **2000**, *83* (4), 825.

of Ti_3Al or the formation of bimetallic nitride and carbide phases of interest for catalysis such as Co_3Mo_3N and Co_3Mo_3C[21] and related phases, from Co−Mo intermetallic phase precursors. In the case of catalysts, a metallic foam or sintered metallic powders could be used as the precursor to achieve the requisite high surface areas, or possibly the use of etching after synthesis to increase surface area, particularly if the ternary nitride/carbide phase was formed as a dispersion in a metallic matrix. Exploration to synthesize and explore previously unknown complex nitride phases, carbide phases, and so forth could be approached, for example, by combinatorial thin or thick film deposition of a range of intermetallic precursor compositions, followed by nitridation reactions, carburization reactions, and so forth. (A two-step process, taking advantage of the precursor intermetallic structure and stoichiometry, rather than a one-step approach, such as is done in reactive sputtering.) A key issue to determine in future work will be the type of complex transition metal nitride (carbide, etc.) phases amenable by this approach, that is, phases in which N or C rest in interstitial sites in a metal alloy dominated by metallic bonding or in a nitrogen array dominated by ionic/covalent bonding.[3]

Conclusions

1. Nitridation of a Cr_3Pt alloy at 1000 °C in pure nitrogen can yield an external, single-phase layer of Cr_3PtN antiperovskite phase if the Cr_3Pt phase composition is sufficiently Cr lean to reflect the 3Cr:1Pt stoichiometry of the antiperovskite. Otherwise, the need to eliminate excess Cr during nitridation results in a discontinuous or cellular type reaction leading to a two-phase lath subscale structure rather than single-phase Cr_3PtN.

2. In two-phase Cr_3Pt dispersed β-Cr alloys, the Cr_3Pt phase composition is Cr-rich and, when nitrided at 1000 °C in pure nitrogen, results in a local cellular type reaction. However, if the Cr_3Pt dispersion is fine enough, the excess Cr can be accommodated by the surrounding β-Cr matrix phase and near single-phase Cr_3PtN can be formed at the Cr_3Pt precipitate sites.

3. Oxidation of intermetallic precursor phases, either as single-phase alloys to yield external layers or as precipitates in two-phase alloys to yield composite structures, holds promise as a method to synthesize complex nitride and related carbide, and so forth, phase near-surface structures.

Acknowledgment. The authors thank Professor Robert Rapp for many helpful discussions on internal and external oxidation and the key issues regarding the formation of ternary phases, Santosh Limaye for insight into complex ceramic phases of technological interest, and Nagraj Kulkarni, Bruce Pint, and Peter Tortorelli for many fruitful discussions and for reviewing this manuscript. This research was sponsored by the U.S. Department of Energy, Fossil Energy Advanced Research Materials (ARM) Program. This work was also supported by the Processing Science Initiative at Ames Laboratory, Office of Basic Energy Sciences, Materials Sciences Division, of the U.S. Department of Energy under Contract No. W-7405-ENG-82. Sarah K. Wrobel was funded by the National Science Foundation (NSF) through an Integrative Graduate Education and Research Training (IGERT) Program (DGE-9987548) under the direction of Professors Peter Liaw and Raymond Buchanan. Oak Ridge National Laboratory is managed by UT-Battelle, LLC, for the U.S. Department of Energy under Contract DE-AC05-00OR22725.

Note Added after ASAP Posting

This article was released ASAP on 4/9/2004 with a misspelling in one of the authors names. The correct version was posted on 4/29/2004.

CM034942P

(21) Korlann, S.; Diaz, B.; Bussell, M. E. *Chem. Mater.* **2002**, *12*, 4049.